

CYP4Fs Expression in Rat Brain Correlates with Changes in LTB₄ Levels after Traumatic Brain Injury

Ying Wang,¹ Jing Zhao,² Auinash Kalsotra,¹ Cheri M. Turman,¹ Raymond J. Grill,³
Pramod K. Dash,^{2,3} and Henry W. Strobel¹

Abstract

Cytochrome P450 (CYP) 4Fs constitute a subgroup of the cytochrome P450 superfamily and are involved in cellular protection and metabolism of numerous molecules, including drugs, toxins, and eicosanoids. CYP4Fs are widely distributed in rat brain with each isoform having a unique distribution pattern throughout different brain regions. The present study shows that traumatic brain injury (TBI) triggers inflammation and elicits changes in mRNA expression of CYP4Fs in the frontal and occipital lobes and the hippocampus. At 24 h post-injury, almost all CYP4F mRNA expression is suppressed compared with sham control throughout these three regions, while at 2 weeks post-injury, all CYP4F mRNAs increase, reaching levels higher than those at 24 h post-injury or uninjured controls. These changes in CYP4F levels inversely correlate with levels of leukotriene B₄ (LTB₄) levels in the brain following injury at the same time points. TBI also causes changes in CYP4F protein expression and localization around the injury site. CYP4F1 and CYP4F6 immunoreactivity increases in surrounding astrocytes, while CYP4F4 immunoreactivity shifts from endothelia of cerebral vessels to astrocytes.

Key words: cytochrome P450 4Fs (CYP4Fs); inflammation; leukotriene B₄ (LTB₄); omega-hydroxylation; traumatic brain injury (TBI)

Introduction

CYTOCHROMES P450 (CYP450s) constitute a superfamily of heme-containing oxidases, most of which are monooxygenases. The substrates of CYP450 include not only xenobiotics such as drugs and toxins, but also endobiotics, including fatty acids, bile acids, eicosanoids, vitamins, cholesterol, and steroids (Andersson et al., 1989; Kikuta et al., 1993; Kawashima et al., 1997; Hoagland et al., 2001; Guengerich, 2003; Cheng et al., 2004). Previous studies have demonstrated that CYP450 enzymes are involved in the resolution of inflammation and infection, and that their expression levels and/or catalytic activities are changed by these pathophysiological processes (Williams, 1991; Nicholson and Renton, 1999). Moreover, the response of CYP450 to inflammation is greatly modulated by cytokines and inflammatory signals, and is dependent to some extent upon the inflammation models used and the CYP450 families studied.

To date, five mouse cytochrome P450 4F (CYP4F) isoforms, four rat isoforms, and six human isoforms have been identified. CYP4F enzymes are expressed in many organs, including the brain (Kawashima and Strobel, 1995). Their distribution patterns and functions in the brain, however, are at the initial stages of investigation. Some CYP4F enzymes are able to metabolize psychoactive drugs such as chlorpromazine (Boehme and Strobel, 2001; Kalsotra et al., 2004) and imipramine (Kawashima et al., 1996). It is quite possible that CYP4Fs serve as an additional metabolic barrier against drugs in the brain in addition to the physiological blood-brain barrier. Therefore, the characterization of CYP4F isoforms expression and distribution in both the intact and injured brain will add to the understanding of their enzymatic function. The CYP4F subfamily also has been shown to catalyze *in vitro* the omega-hydroxylation of endogenous eicosanoids such as leukotriene B₄ (LTB₄) (Jin et al., 1998; Bylund et al., 2003), arachidonic acid (Hoagland et al., 2001; Lasker et al., 2000), and prostaglandin A₁ and E₁ (Kawashima

Departments of ¹Biochemistry and Molecular Biology, ²Neurobiology and Anatomy, and ³Neurosurgery, Vivian L. Smith Center for Neurological Research, University of Texas-Houston Medical School, Houston, Texas.

et al., 1997). These eicosanoids are important inflammatory molecules, and their metabolism by the CYP4F subfamilies inactivates them as inflammatory signaling molecules, indicating that CYP4Fs may play a role in the resolution of inflammation.

Traumatic brain injury (TBI) is a major public health problem and can lead to lethal multiple organ dysfunction syndrome, in which acute systemic inflammation plays an essential role (Faden et al., 1989; McIntosh, 1994; Ott et al., 1994). A previous study from our laboratory (Cui et al., 2003) indicated that rat CYP4F4 and CYP4F5 gene expression in hippocampus was modulated in a time-dependent fashion after TBI, indicating a potential role for CYP4Fs in inflammation following TBI. We hypothesize that CYP4Fs are widely distributed in the brain and that TBI can induce broader changes of CYP4Fs expression in multiple brain regions. It is important to know how CYP4Fs expression varies during brain inflammation post-TBI in order to predict the effects of brain injury on drug metabolism in the brain, identify means to enhance recovery post injury, and regulate inflammatory mediator levels by modulation of CYP4Fs activity.

Methods

All chemicals utilized, if not specifically defined, were of reagent grade quality or higher.

Brain injury

Male Sprague Dawley rats (250–300 g body wt) were purchased from Harlan Laboratories (Indianapolis, IN). All protocols were conducted in compliance with guidelines set forth in the *NIH Guide for the Care and Use of Laboratory Animals* and approved by the University of Texas Health Science Center's Institutional Animal Care and Use Committee. Rats were initially anesthetized using 5% isoflurane with a 1:1 N₂O/O₂ mixture and then maintained with 2.5% isoflurane with a 1:1 N₂O/O₂ mixture via face mask. Animals were mounted on the stereotaxic frame secured by ear bars and an incisor bar. Rats received a single, unilateral impact at 6 m/sec, 2.5-mm deformation performed midway between the bregma and the lambda with the edges of craniotomies 1 mm lateral to the midline. The brains of sham-operated but uninjured rats served as controls. Core body temperature was monitored continuously by a rectal thermometer and maintained at 36–36.5°C. After injury, the scalp was sutured and closed. The animals were sacrificed at different time points (24 h and 2 weeks) after the injury.

Microsome and RNA preparations

After animals were sacrificed, microsomes from frontal lobe, frontal cortex, occipital lobe, hippocampus, cerebellum, striatum, midbrain and medulla were prepared by differential centrifugation as described by Saito and Strobel (1981). All procedures were carried out at 4°C. The separated brain tissues were washed and homogenized in 6 volumes of homogenization buffer (20 mM potassium phosphate buffer, 1 mM EDTA, 0.25 mM sucrose, pH 7.2–7.4) with Complete Protease Inhibitor Cocktail Tablets (2 tablets/100 mL buffer, Roche Inc.). Each homogenate was centrifuged at 3,220×g for 20 min, and the supernatant fraction was collected. The

supernatant fraction was further centrifuged at 105,000×g for 60 min. After centrifugation, the supernatant fraction was discarded and the pellet was homogenized and washed in homogenization buffer without protease inhibitors, and centrifuged again at 105,000×g for 60 min. The final pellets were resuspended in homogenization buffer without protease inhibitors and stored at –80°C for further analysis. The microsomal protein concentrations were determined using the bicinchoninic acid procedure (Smith et al., 1985). Brain regions frontal lobe, hippocampus, and occipital lobe from the ipsilateral hemisphere were separated and stored at –80°C for RNA isolation. Total RNA was isolated according to the methods of Chomczynski (1993).

Quantitative real-time polymerase chain reaction

All samples were DNase-treated using RQ1 DNase (Promega, Madison, WI). The quality of the isolated RNA was assessed by electrophoresis on 1% agarose gels based on the integrity of 28s and 18s ribosomal RNA bands after ethidium bromide staining. Polymerase chain reaction (PCR) primers and fluorescent probe sequences for CYP4F isoforms were utilized as reported previously (Kalsotra et al., 2002). Aliquots (200 ng) of total RNA were reverse transcribed in triplicate, including a real-time (RT) blank to account for amplification of any contaminating genomic DNA. Amplification was performed using an ABI Prism 7700 (Applied Biosystems, Norwalk, CT) at 95°C for 1 min, followed by 40 cycles at 95°C for 12 sec and 60°C for 1 min. Standard curves were generated by plotting Ct versus the log of the amount of amplicon (custom made by IDT, Coralville, IA) for specific CYP4Fs (500ag–5pg), and were used to compare the relative amount of each CYP4F mRNA in the samples.

Enzyme-linked immunosorbent assay for LTB₄

The leukotriene B₄ (LTB₄) level from each specific brain region (frontal lobe, hippocampus or occipital bulb) was below the detectable range of this enzyme-linked immunosorbent assay (ELISA). Therefore, the injured rat cerebral hemispheres (excluding the cerebellum, medulla, and olfactory lobe) were separated from the contralateral side to determine LTB₄ levels in triplicate by a commercially available competitive enzyme immunoassay kit utilizing reagents and procedures provided by Cayman Chemicals Co. (Ann Arbor, MI). The absorbance was read at 410 nm on a Dynex ELISA reader.

CYP4F4 and CYP4F6 antibody design

CYP4F1 and CYP4F5 antibodies are gifts from Dr. Yasushi Kikuta's laboratory (Fukuyama, Japan). CYP4F4 and CYP4F6 antibodies were generated by our laboratory using synthetic peptides. Sequences were selected by first preparing a multiple sequence alignment of rat CYP4Fs to determine regions of high sequence uniqueness using CLUSTALW. Next, a three-dimensional (3D) homology model of each cytochrome P450 was simulated by sequence fitting in Swiss PDB Viewer 3.7 to the template structures P450 BM3 (2HPD), P450 terp (1CPT), and P450 2C5 (1DT6) available as PDB files from Brookhaven Protein Data Bank. Candidate peptide sequences chosen from the homology models were then tested for synthetic feasibility using the program Pinsoft32 (2.11)

from Chiron Technologies. As a final screen, each of the selected peptides was BLAST-searched against all non-redundant GenBank CDS translations, PDB, SwissProt, PIR, and PRF databases using NCBI BLAST. The only significant cross-reaction for each of the peptides selected was with the mouse orthologue. The final sequences we selected to develop CYP4F4 and CYP4F6 antipeptide antibodies are 236-YQQLLLHTDSL-246 and 64-TLMKNNEEGMQFIAHLGRN-83, respectively. These peptides were used to generate rabbit polyclonal antibodies. The antiserum was affinity-purified using the affinity gel attached with the above antipeptides respectively to improve the specificity of each antibody.

Western blotting

Microsomal protein samples extracted from different normal rat brain regions including the frontal lobe, frontal cortex, occipital lobe, hippocampus, cerebellum, striatum, midbrain, and medulla were boiled in Laemmli buffer and resolved on 4–15% gradient Tris-glycine sodium dodecyl sulfate–polyacrylamide gel electrophoresis (SDS-PAGE) gels. Proteins were transferred to PVDF membranes using a semi-dry transfer apparatus. Membranes were blocked for 1 h at room temperature with 5% dried non-fat milk followed by overnight incubation at 4°C in antibodies (1:1000 dilution) against CYP4F1, 4F4, 4F5, or 4F6. Membranes were then washed and incubated at room temperature with horseradish peroxidase (HRP)–conjugated secondary antibody (1:1000 dilution) for 1 h. Immunoreactivity was detected using a HRP chemiluminescence system (Pierce, Rockford, IL).

Immunohistochemistry assay

Expression and localization of CYP4F1, 4F4, and 4F6 in rat brain tissues were examined by immunofluorescence analysis. Two animals at sham, 24 h post-injury, or 2 weeks post-injury were euthanized and transcardially perfused with 4% paraformaldehyde in 0.1 M PBS. Following perfusion, the brains were removed and post-fixed overnight in 4% paraformaldehyde, and then transferred into 30% sucrose in PBS for cryoprotection for a period of at least 72 h. The brains were then cut in the coronal plane on a cryostat (Reichardt-Jung), generating tissue sections at a thickness of 40 μ m. The free-floating sections were blocked with 5% normal goat serum in 1 \times Tris-buffered saline (TBS) and permeabilized with 0.25% TBS. Triton X-100 in Gross lesion morphology was assessed in every sixth tissue section labeled with thionin to detect Nissl substance. Thionin-stained slides were placed into a Pathscan Enabler (Meyer Instruments, Houston, TX) holder and imaged using a Kodak (Rochester, NY) slide-scanner. Scanned images were manipulated in Adobe Photoshop to enhance contrast. Cellular localization of CYP4Fs was performed using triple-label immunofluorescence. Two tissue sections across the injury site were chosen per animal were incubated with the primary antibodies, i.e., rabbit anti-rat CYP4F antibody (1:1000 dilution), mouse anti-rat endothelial cellular antigen-1 (RECA-1, 1:50 dilution), and guinea pig anti-rat glial fibrillary acidic protein (GFAP, 1:500 dilution) at 4°C for 48 h and washed in 1 \times TBS three times for 10 min each, and then incubated with the appropriate Alexafluor-linked secondary antibodies at 488-, 568-, 647-nm (1:500 dilution, Molecular Probes) for 3 h at room temperature. After the sections were washed in 1 \times TBS

three times for 10 min each, they were mounted on slides and dried at room temperature. The sections were coverslipped with Fluormount-G (Fisher Scientific) to retard fading. Fluorescent images were collected using a three-line confocal microscope (BioRad Radiance 2000 system attached to an Olympus BX-50 microscope). The laser power, iris settings, and gain were kept constant between injured and sham brain sections. Final images were processed in Adobe Photoshop 7.0.

Statistical analysis

One-way analysis of variance (ANOVA) followed by Tukey's multiple comparison test was used for the statistical analysis.

Results

Regional distribution of CYP4F proteins in sham samples

The immunoblot data shown in Figure 1 demonstrate that the protein expression levels of the various CYP4Fs isoforms vary considerably among the different brain regions examined, i.e., frontal lobe, frontal cortex, occipital lobe, cerebellum, striatum, midbrain, and medulla. CYP4F4 and 4F6 are in general more widely distributed than CYP4F1 and 4F5 in these brain regions. CYP4F1 protein is expressed at the lowest level; only the frontal lobe and the occipital lobe show positive CYP4F1 immunoreactivity. CYP4F5 shows immunoreactivity in most brain regions except for the cerebellum, midbrain, and medulla. Compared with other brain regions, the occipital lobe followed by the frontal lobe have the highest level of CYP4Fs protein expression relative to the other region examined. In the medulla, all CYP4Fs immunoreactivity is barely detected by Western blot analysis.

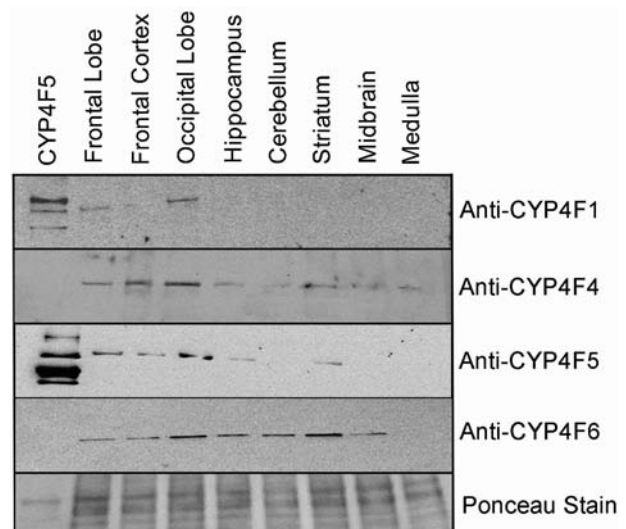


FIG. 1. Western blotting analysis of CYP4F proteins expression in different parts of normal rat brain. Microsomes were isolated from each brain part, as described in Methods. 60 μ g of microsomal proteins from each sample was separated electrophoretically and transferred onto nitrocellulose or PVDF membrane. Membranes were blotted and analyzed using anti-CYP4F1, anti-CYP4F4, anti-CYP4F5, and anti-CYP4F6 antibodies.

Temporal changes in mRNA levels of CYP4Fs in three different brain regions after TBI

As shown in Figure 2a–c, compared with sham samples, all CYP4F mRNA levels in the frontal lobe, hippocampus and occipital lobe, tend to decrease first and then increase as a function of time after TBI. The mRNA levels of CYP4F1 and CYP4F4 in these three regions have a more dramatic response to the injury as compared to those of CYP4F5 and CYP4F6. In the frontal lobe, CYP4F1, 4F4, 4F5, and 4F6 mRNA levels at 24 h post-injury decline by 88.9%, 76.8%, 46.7%, and 40.3%, respectively, as compared to the relative sham level. At 2 weeks post-injury, the mRNA level of each isoform returns to the sham level. Similar post-injury change patterns of mRNA expression levels occur in the hippocampus for each CYP4F isoform (Fig. 2b). The obvious difference in the hippocampus is that CYP4F5 level at 24 h post-injury does not decrease significantly compared with the sham level. In the occipital lobe (Fig. 2c), the decreasing mRNA expression patterns of all four isoforms at 24 h post-injury are similar to those in the frontal lobe. At 2 weeks post-injury, CYP4F mRNA levels increase but do not reach the original sham level.

Temporal changes in the rat brain LTB_4 level after TBI

The ELISA data in Figure 2d indicate that the LTB_4 level in the sham rat brain is about 74 pg/gram tissue. At 24 h post-injury, the LTB_4 level significantly increases to 119 pg/gram tissue in the ipsilateral cerebral hemisphere of rat brain. At 2 weeks post-injury, the LTB_4 level greatly decreases to about 54 pg/gram tissue.

Changes in CYP4F protein expression and localization around the injury site after TBI

In the area delineated by the red box of Figure 3a, including dorsal hippocampus, corpus callosum, and ventral

cortex of the sham brain slice (representing areas directly affected by cortical contusion injury), very little CYP4F1 (Fig. 3b) protein is detected via immunohistochemistry. The few cells that demonstrate CYP4F1 immunoreactivity colocalize with glial fibrillary acidic protein (GFAP), the chief intermediate filament protein expressed by astrocytes in the CNS (Fig. 3c–e). A higher level of CYP4F1 protein expression is present on the cortical surface of the brain, where CYP4F1 immunoreactivity also colocalizes with GFAP (data not shown), most likely recognizing astrocytes comprising the glia limitans. At 24 h post-injury, greater numbers of CYP4F1-immunoreactive (IR) cells can be detected in the tissue bordering the lesion site (Fig. 3h). All of these CYP4F1-IR cells are identified as astrocytes since they co-express GFAP (Fig. 3h–j). RECA-1-labeled slides are shown in Figure 3e,g,j,o in order to determine that CYP4F1 is not expressed the endothelial cells although isoform-specific expression of CYP4F4 protein was detected in blood vessels as we are going to describe below. At 2 weeks post-injury, CYP4F1 protein expression is much higher around the injury site (Fig. 3l) and continues to be associated with astrocytes (Fig. 3m–o).

Figure 4 illustrates the changes of CYP4F4 protein expression. In the sham brain section, CYP4F4 expression is present in the representative region (Fig. 3a, labeled in the red box in Fig. 4a) as shown in Figure 4b,d; it is colocalized with the RECA-1-labeled endothelial cells of brain blood vessels (Fig. 4b–e), while at the edge of the brain slice, CYP4F4 is also present in boundary astrocytes (data not shown). At 24h post injury, it is hard to tell whether CYP4F4 protein expression remains at the same level as in the sham slice or changes slightly (Fig. 4g), but CYP4F4 is no longer detected within the blood vessels bordering the injury site. Instead, CYP4F4-IR is now associated with astrocytes at the lesion border (Fig. 4h–j). While CYP4F4 expression at the lesion site is no longer vascular, within around 300 μ m from the injury site, expression is still endothelial. At 2 weeks post-injury,

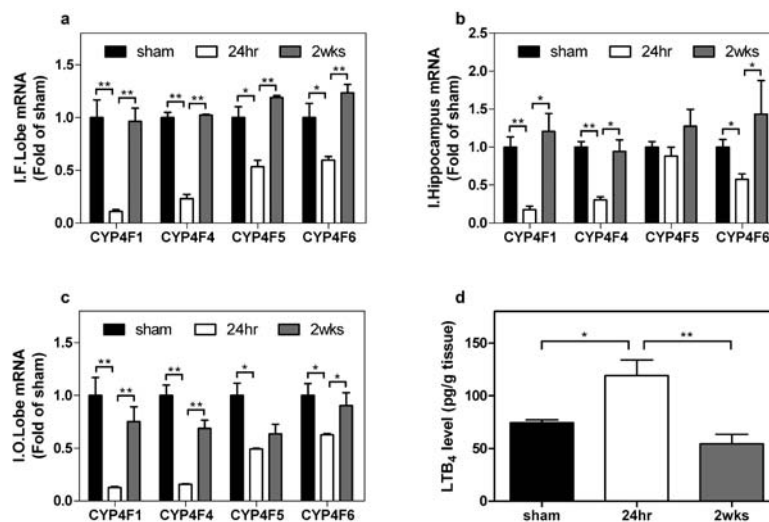


FIG. 2. CYP4Fs mRNA and LTB_4 quantitation in rat brain after brain injury. Time course for changes in CYP4F1, CYP4F4, CYP4F5, and CYP4F6 in the frontal lobe (a), hippocampus (b), and occipital lobe (c) of the ipsilateral side. Rats were treated as described in Methods. Each data point represents $n = 5$. The expression of CYP4Fs was quantitated by QRT-PCR. (d) EIA-based brain LTB_4 estimation after injury. Each data point represents $n = 3$. * $p < 0.05$, ** $p < 0.01$ compared with 24-h post-injury.

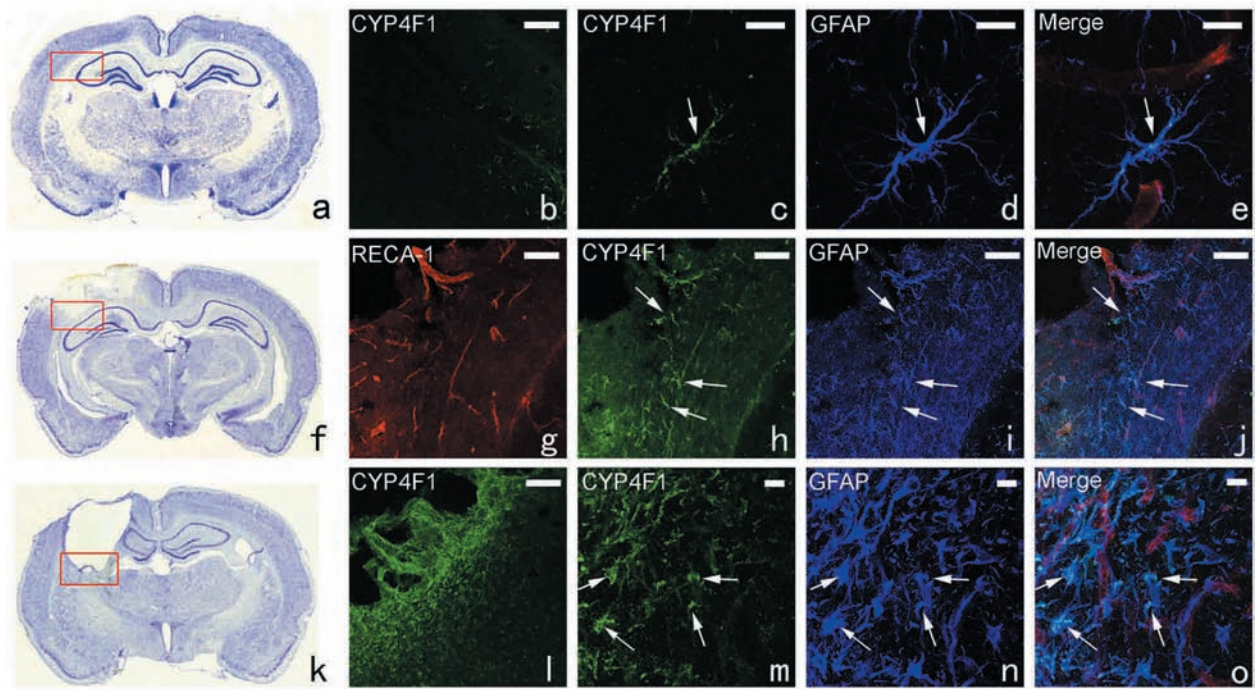


FIG. 3. Immunohistochemical analysis of CYP4F1 protein expression and distribution in the rat brain. Free-floating tissue sections were labeled with RECA-1 (red), GFAP (blue), and CYP4F1 antibody (green). (a,f,k) Nissl's stained brain sections for sham, 24 h post-injury, and 2 weeks post-injury, respectively. Immunofluorescence confocal microscopy was focused on the regions labeled with red rectangles. (b-e,g-j,l-o) 4F1 protein expression and localization at sham, 24 h post-injury, and 2 weeks post-injury, respectively. (b,h,l) Low magnification to show the distribution of CYP4F1 around the injury site. Arrows in c-e,h-j,m-o indicate the colocalization of CYP4F1 with astrocytes. Scale bar = 25 μ m (b,g-j,l), 10 μ m (c-e,m-o).

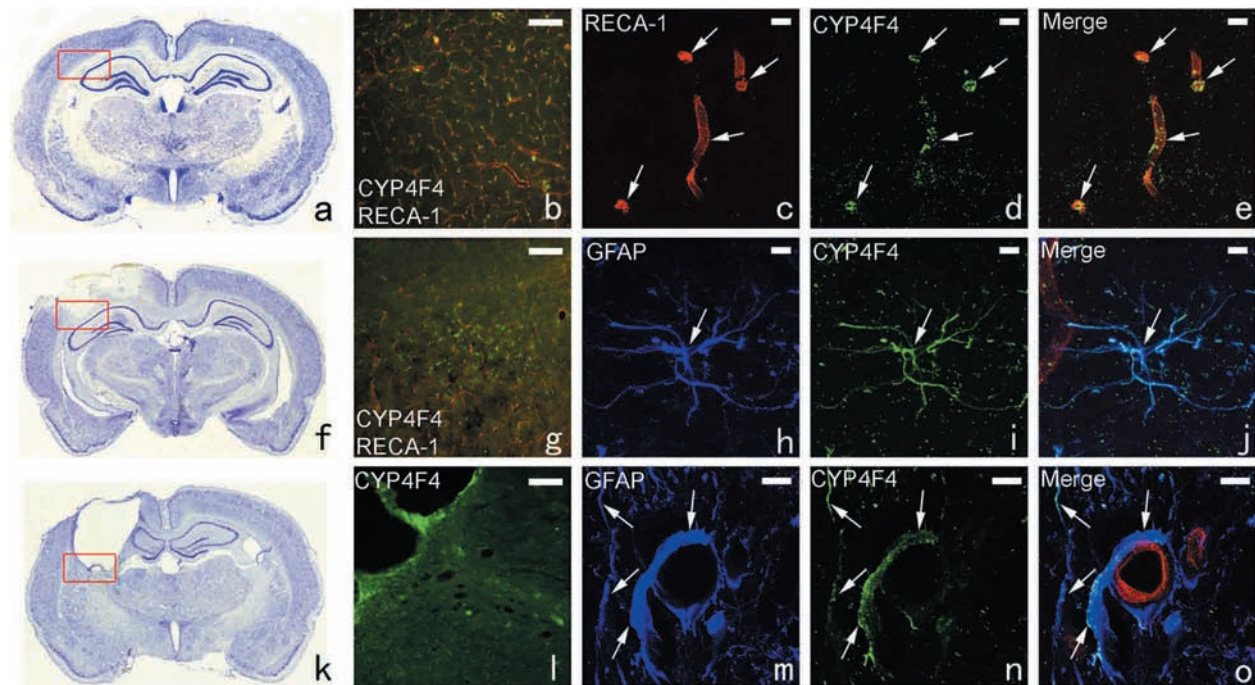


FIG. 4. Immunohistochemical analysis of CYP4F4 protein expression and distribution in the rat brain. Free-floating tissue sections were labeled with RECA-1 (red), GFAP (blue), and CYP4F4 antibody (green). (a,f,k) Nissl's stained brain sections at sham, 24 h post-injury, and 2 weeks post-injury, respectively. Immunofluorescence confocal microscopy was focused on the regions labeled with red rectangles. (b-e,g-j,l-o) 4F4 protein expression and localization at sham, 24 h post-injury, and 2 weeks post-injury, respectively. (b,g,l) Low magnification to show the distribution of CYP4F4 around the injury site. Arrows in c-e indicate the colocalization of CYP4F4 with endothelial cells of blood vessels. Arrows in h-j,m-o indicate colocalization of CYP4F4 with astrocytes. Scale bar = 50 μ m (b,g,l), 10 μ m (c-e,h-j,m-o).

CYP4F4 protein expression is concentrated at the edge of the injury site (Fig. 4l). The high-magnification pictures (Fig. 4m–o) show that CYP4F4 is colocalized with astrocytes.

As for CYP4F6 protein, no signal is detected in the representative region of the sham section (Fig. 5b). The expression is detected at the outer surface of the rat brain as indicated in the blue box in Figure 5a and is colocalized with astrocytes of the glia limitans (Fig. 5c–e). At 24 h post-injury, CYP4F6 protein expression is induced (Fig. 5h) around the injury site and the protein is localized in the astrocytes (Fig. 5g–j). At 2 weeks post-injury, CYP4F6 expression remains concentrated around the injury site (Fig. 5l) and associated with astrocytes (Fig. 5m–o). Compared with the region around the lesion site, the expression levels and localization of all CYP4F proteins on the uninjured contralateral side show the same patterns of expression as those in sham animals (data not shown).

Sections incubated with the same three fluorescence-tagged secondary antibodies without primary antibodies were used as the negative controls. As shown in Supplemental Figure 1, no detectable signal was found on those sections.

Discussion

Injury to the mammalian CNS results in drastic cellular inflammatory reactions, which includes the breakdown of phosphatidylinositol biphosphate into diacylglycerol (DAG) and inositol tris-phosphate (IP₃) by phospholipase C (Cartier et al., 2005). IP₃ generation leads to a dramatic increase in intracellular calcium concentration, which as a con-

sequence activates calcium dependent Phospholipase A₂. Phospholipase A₂ hydrolyzes phospholipids such as phosphatidylcholine, thereby generating arachidonic acid, a precursor substrate for inflammatory mediators, while DAG lipase serves as the second source of arachidonic acid formation through enzymatic breakdown of DAG. Arachidonic acid can be readily utilized by 5-lipoxygenase (5-LOX) and cyclooxygenase-2 (COX-2) to generate leukotrienes or prostaglandins, respectively. Leukotrienes and prostaglandins are potent vasoactive mediators of inflammation and can be shuttled out of the cell to the extracellular space by specific transporters. The injury induced brain inflammation is characterized by activation of astrocytes. The essential role of reactive astrocytes in TBI has been further confirmed by a recent finding that transgenically targeted ablation of proliferating reactive astrocytes leads to exacerbated neuronal degeneration and inflammation after a moderate controlled cortical impact in mouse brain (Myer et al., 2006). Together with the astrocyte reaction, injury to the brain also leads to the breakdown/compromise of the blood-brain barrier, resulting in extravasation or recruitment of immune cells such as neutrophils, macrophages, monocytes, eosinophils, B cells and T cells, ions, and other plasma components resulting in the subsequent formation of vasogenic edema. Also, the cytokines (especially IL-1, IL-6, and TNF- α) released by these immune cells by activated and degranulating macrophages can amplify the inflammatory signal many-fold (Ghirnikar et al., 1998).

CYP4Fs might serve a protective role in TBI by resolving inflammation since they catalyze ω -hydroxylation of the potent inflammatory mediators LTB₄, PGA₁, and PGE₁ to their

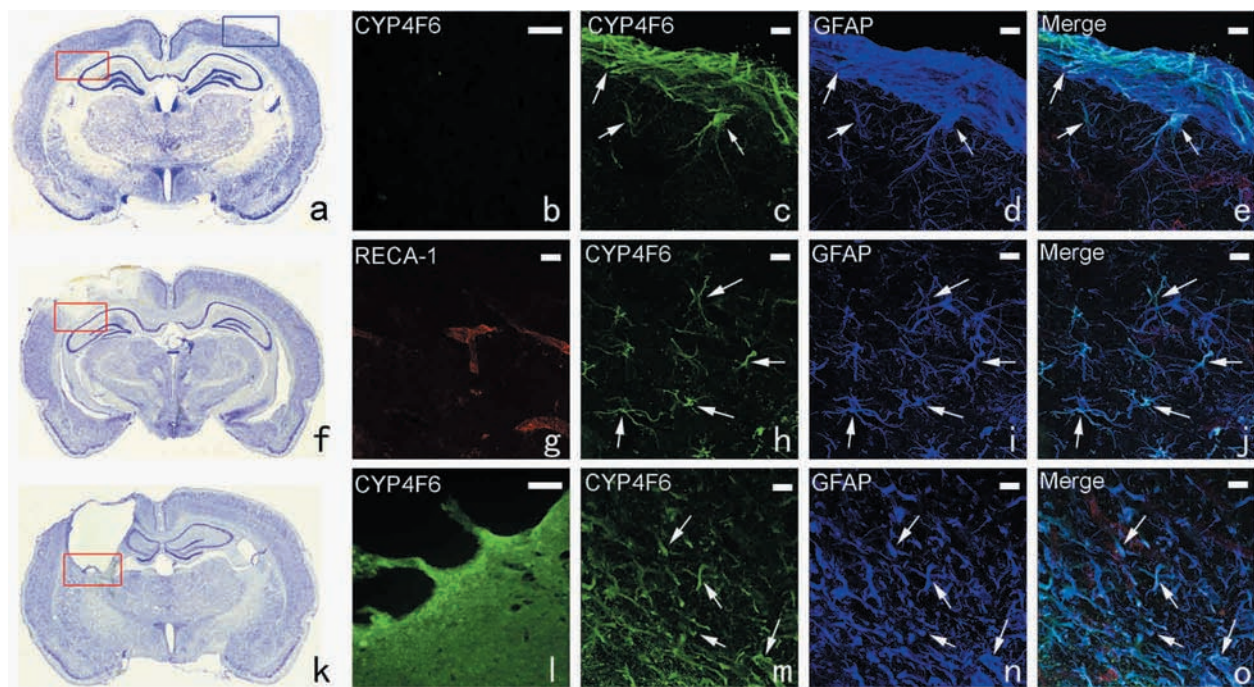


FIG. 5. Immunohistochemical analysis of CYP4F6 protein expression and distribution in the rat brain. Free-floating tissue sections were labeled with RECA-1 (red), GFAP (blue), and CYP4F6 antibody (green). (a,f,k) Nissl's stained brain sections at sham, 24 h post-injury, and 2 weeks post-injury, respectively. Immunofluorescence microscopy and confocal microscopy was focused on the region labeled with the rectangle for c–e, while the other immunofluorescent figures were focused on the regions labeled with red rectangles. (b,l) Low magnification to show the distribution of CYP4F6 around the injury site. Arrows in c–e,h–j,m–o indicate the colocalization of CYP4F6 with astrocytes. Scale bar = 50 μ m (b,g,l), 10 μ m (c–e,h–j,m–o).

inactive products, which are incapable of promoting chemotaxis, recruitment of immune cells and formation of edema. TBI brings about a significant decline of CYP4F RNA expression in three different brain regions examined at 24 h post-injury. According to Morgan's theory of P450 down-regulation following inflammation (Morgan, 2001), CYP4F suppression might be part of a pathophysiological response to stress signals of inflammation. Since CYP4Fs may promote the production of reactive oxygen species and catalyze the formation of epoxyeicosatrienoic acids (EETs) that inhibit inflammation, the suppression of CYP4Fs during inflammation immediately after TBI, not only protects brain cells from the harmful oxidative stress, but also prevents EETs inhibition of the host inflammatory response. After the initial decline in expression levels, the expression returns closely to the original level in three regions at 2 weeks post-injury. Our ELISA data show that the LTB₄ level changes in an inverse manner compared with CYP4Fs. The changing pattern of cerebral LTB₄ level is consistent with the temporal profiles of LTB₄ level in the rat cerebrospinal fluid following experimental brain injury as reported by Schuhmann et al. (2003). Changes in CYP4Fs mRNA level also match well with previous studies in other similar traumatic CNS injury models, which showed that injury immediately leads to inflammation involving increased concentrations of leukotrienes and prostaglandins, while after injury, the amount of leukotrienes and prostaglandins begin to decline (Ellis et al., 1981; Shohami et al., 1987; Xu et al., 1990). In the current study CYP4F levels are decreased at 24 h post-TBI, potentially resulting in sufficient levels of LTB₄ to elicit the inflammatory response that is necessary to recruit immune cells and eliminate damaged tissue debris (Butterfield et al., 2006). At 2 weeks post-injury, CYP4F levels dramatically increase in injured brain tissue. One potential role for this increase might be to suppress LTB₄ levels to obviate the possibility that an expanded inflammatory response would damage the normal tissue.

It is possible that leukotrienes and prostaglandins are not the only mediators through which CYP4Fs function in brain inflammation. Previous studies have indicated that CYP4F1 and CYP4F4 catalyze the omega-hydroxylation of arachidonic acid to 20-HETE (Xu et al., 2004), an anti-inflammatory vasoconstrictor. According to the study of Poloyac et al. (2006), systemic 20-HETE inhibition by HET0016 is beneficial acutely after temporary middle cerebral artery occlusion in rats. As shown in the present study, CYP4F1 and CYP4F4 are more dramatically reduced in mRNA levels compared with CYP4F5 and CYP4F6 at 24 h post-injury, indicating that the acute reduction of CYP4Fs mRNA level may be beneficial via the reduction of 20-HETE formation. Therefore, CYP4Fs may also function by production of 20-HETE. More studies are needed to provide insight into the mechanism of how the CYP4Fs genes are suppressed after inflammation and then induced during the recovery state. All four rat CYP4F isoforms can metabolize LTB₄, while little is known about the substrate specificity of each isoform. Selective inhibition of CYP4F isoforms followed by careful biochemical and neuroanatomical studies is also necessary to define further the potential role of CYP4Fs in brain trauma.

The immunofluorescence data demonstrate that TBI can cause changes in the expression and localization of CYP4F1, 4F4, and 4F6 around the injury site. CYP4F1 and CYP4F6 localize in the astrocytes and their expression around the injury site has a time-course of increase after TBI consistent

with the TBI-induced astrocyte activation. In contrast, the immunofluorescence profile of both isoforms on the contralateral side does not significantly change compared with the sham control sample. This seems to be a regional response to TBI in order to regulate the inflammation caused by the injury through the metabolism of LTB₄ as we described above. Most interestingly, the primary site of CYP4F4 protein localization around the injury site changes from the endothelia of cerebral microvessels before TBI to the astrocytes after TBI. It is not realistic to expect that CYP4F4 protein migrates from cerebral microvessels to astrocytes. It seems that around the injury site, CYP4F4 protein expression is downregulated in the endothelia and modulated upward in the astrocytes. From Figure 4o, we find that there is an obvious gap, most likely the basal lamina of the blood-brain barrier, on and through which astrocytic endfeet are found. As shown in the study of Xu et al. (2004), CYP4F4 and CYP4F1 catalyze the omega-hydroxylation of arachidonic acid with similar k_{cat} values (11 min⁻¹ and 9 min⁻¹, respectively), producing 20-HETE. 20-HETE is not only a vasoconstrictor but also a second messenger of angiogenesis mediated by VEGF (Amaral et al., 2003; Jiang et al., 2004). Occurrence of angiogenesis has been documented as an important recovery process after traumatic brain injury (Frontczak-Baniewicz et al., 2002). 20-HETE has a potential role in angiogenesis as vascular remodeling clearly occurs following TBI. Thus, except for their possible function in the inhibition of inflammation by metabolizing LTB₄, CYP4F4, and CYP4F1, which are induced in astrocytes around the injury site, may also function in angiogenesis in the injury region. This may partly explain why CYP4F4 shows a change in its localization site from endothelia to astrocytes and why the CYP4F1 remains elevated around the lesion site during the recovery state.

Acknowledgments

This work was supported by NINDS (grants NS44174 to H.W.S., NS35457 to P.K.D., and NS049409 to R.J.G.) and the Department of the Army (T5 grant to H.W.S.).

Author Disclosure Statement

No competing financial interests exist.

References

- Amaral, S.L., Maier, K.G., Schippers, D.N., Roman, R.J., and Greene, A.S. (2003). CYP4A metabolites of arachidonic acid and VEGF are mediators of skeletal muscle angiogenesis. *Am. J. Physiol. Heart Circ. Physiol.* 284, 1528–1535.
- Andersson, S., Davis, D.L., Dahlback, H., Jornvall, H., and Russell, D.W. (1989). Cloning, structure, and expression of the mitochondrial cytochrome P-450 sterol 26-hydroxylase, a bile acid biosynthetic enzyme. *J. Biol. Chem.* 264, 8222–8229.
- Boehme, C.L., and Strobel, H.W. (2001). In vitro metabolism of chlorpromazine by cytochrome P4504F4 and 4F5 and the inhibitory effect of imipramine. *Neurotoxicity Res.* 3, 329–337.
- Butterfield, T.A., Best, T.M., and Merrick, M.A. (2006). The dual roles of neutrophils and macrophages in inflammation: a critical balance between tissue damage and repair. *J. Athl. Train.* 41, 457–465.
- Bylund, J., Harder, A.G., Maier, K.G., Roman, R.J., and Harder, D.R. (2003). Leukotriene B4 omega-side chain hydroxylation by CYP4F5 and CYP4F6. *Arch. Biochem. Biophys.* 412, 34–41.

- Cartier, L., Hartley, O., Dubois-Dauphin, M., and Krause, K.H. (2005). Chemokine receptors in the central nervous system: role in brain inflammation and neurodegenerative diseases. *Brain Res. Brain Res. Rev.* 48, 16–42.
- Cheng, J.B., Levine, M.A., Bell, N.H., Mangelsdorf, D.J., and Russell, D.W. (2004). Genetic evidence that the human CYP2R1 enzyme is a key vitamin D 25-hydroxylase. *Proc. Natl. Acad. Sci. USA* 101, 7711–7715.
- Chomczynski, P. (1993). A reagent for the single-step simultaneous isolation of RNA, DNA and proteins from cell and tissue samples. *Biotechniques* 15, 532–534, 536–537.
- Cui, X., Kalsotra, A., Robida, A.M., Matzilevich, D., Moore, A.N., Boehme, C.L., Morgan, E.T., Dash, P.K., and Strobel, H.W. (2003). Expression of cytochromes P450 4F4 and 4F5 in infection and injury models of inflammation. *Biochim. Biophys. Acta* 1619, 325–331.
- Ellis, E.F., Wright, K.F., Wei, E.P., and Kontos H.A. (1981). Cytochrome products of arachidonic acid metabolism in cat cerebral cortex after experimental concussive brain injury. *J. Neurochem.* 37, 892–896.
- Faden, A.I., Demediuk, P., Panter, S.S., and Vink, R. (1989). The role of excitatory amino acids and NMDA receptors in traumatic brain injury. *Science* 244, 798–800.
- Frontczak-Baniewicz, M., and Walski, M. (2002). Non-sprouting angiogenesis in neurohypophysis after traumatic injury of the cerebral cortex. *Electron-microscopic studies. Neurol. Endocrinol. Lett.* 23, 396–404.
- Ghimrikar, R.S., Lee, Y.L., and Eng, L.F. (1998). Inflammation in traumatic brain injury: role of cytokines and chemokines. *Neurochem. Res.* 23, 329–340.
- Guengerich, F.P. (2003). Cytochromes P450, drugs, and diseases. *Mol. Interv.* 3, 194–204.
- Hoagland, K.M., Maier, K.G., Moreno, C., Yu, M., and Roman, R.J. (2001). Cytochrome P450 metabolites of arachidonic acid: novel regulators of renal function. *Nephrol. Dial. Transplant.* 16, 2283–2285.
- Jiang, M., Mezentsev, A., Kemp, R., Byun, K., Falck, J.R., Miano, J.M., Nasjletti, A., Abraham, N.G., and Laniado-Schwartzman, M. (2004). Smooth muscle-specific expression of CYP4A1 induces endothelial sprouting in renal arterial microvessels. *Circ. Res.* 94, 167–174.
- Jin, R., Koop, D.R., Raucy, J.L., and Lasker, J.M. (1998). Role of human CYP4F2 in hepatic catabolism of the proinflammatory agent leukotriene B₄. *Arch. Biochem. Biophys.* 359, 89–98.
- Kalsotra, A., Anakk, S., Boehme, C.L., and Strobel, H.W. (2002). Sexual dimorphism and tissue specificity in the expression of CYP4F forms in Sprague Dawley rats. *Drug Metab. Dispos.* 30, 1022–1028.
- Kalsotra, A., Turman, C.M., Kikuta, Y., and Strobel, H.W. (2004). Expression and characterization of human cytochrome P450 4F11: Putative role in the metabolism of therapeutic drugs and eicosanoids. *Toxicol. Appl. Pharmacol.* 199, 295–304.
- Kawashima, H., and Strobel, H.W. (1995). cDNA cloning of three new forms of rat brain cytochrome P450 belonging to the CYP4F subfamily. *Biochem. Biophys. Res. Commun.* 217, 1137–1144.
- Kawashima, H., Sequeira, D.J., Nelson, D.R., and Strobel, H.W. (1996). Genomic cloning and protein expression of a novel rat brain cytochrome P-450 CYP2D18* catalyzing imipramine N-demethylation. *J. Biol. Chem.* 271, 28176–28180.
- Kawashima, H., Kusunose, E., Thompson, C.M., and Strobel, H.W. (1997). Protein expression, characterization, and regulation of CYP4F4 and CYP4F5 cloned from rat brain. *Arch. Biochem. Biophys.* 347, 148–154.
- Kikuta, Y., Kusunose, E., Endo, K., Yamamoto, S., Sogawa, K., Fujii-Kuriyama, Y., and Kusunose, M. (1993). A novel form of cytochrome P-450 family 4 in human polymorphonuclear leukocytes. cDNA cloning and expression of leukotriene B₄ omega-hydroxylase. *J. Biol. Chem.* 268, 9376–9380.
- Lasker, J.M., Chen, W.B., Wolf, I., Blosswick, B.P., Wilson, P.D., and Powell, P.K. (2000). Formation of 20-hydroxyeicosatetraenoic acid, a vasoactive and natriuretic eicosanoid, in human kidney. Role of Cyp4F2 and Cyp4A11. *J. Biol. Chem.* 275, 4118–4126.
- McIntosh, T.K. (1994). Neurochemical sequelae of traumatic brain injury: therapeutic implications. *Cerebrovasc. Brain Metab. Rev.* 6, 109–162.
- Morgan, E.T. (2001). Regulation of cytochrome p450 by inflammatory mediators: why and how? *Drug Metab. Dispos.* 29, 207–212.
- Myer, D.J., Gurkoff, G.G., Lee, S.M., Hovda, D.A., and Sofroniew, M.V. (2006). Essential protective roles of reactive astrocytes in traumatic brain injury. *Brain* 129, 2761–2772.
- Nicholson, T.E., and Renton, K.W. (1999). Modulation of cytochrome P450 by inflammation in astrocytes. *Brain Res.* 827, 12–18.
- Ott, L., McClain, C.J., Gillespie, M., and Young, B. (1994). Cytokines and metabolic dysfunction after severe head injury. *J. Neurotrauma* 11, 447–472.
- Poloyac, S.M., Zhang, Y., Bies, R.R., Kochanek, P.M., and Graham, S.H. (2006). Protective effect of the 20-HETE inhibitor HET0016 on brain damage after temporary focal ischemia. *J. Cereb. Blood Flow Metab.* 26, 1551–1561.
- Saito, T., and Strobel, H.W. (1981). Purification to homogeneity and characterization of a form of cytochrome P-450 with high specificity for benzo[alpha]pyrene from beta-naphthoflavone-pretreated rat liver microsomes. *J. Biol. Chem.* 256, 984–988.
- Schuhmann, M.U., Mokhtarzadeh, M., Stichtenoth, D.O., Skardelly, M., Klinge, P.M., Gutzki, F.M., Samii, M., and Brinker, T. (2003). Temporal profiles of cerebrospinal fluid leukotrienes, brain edema and inflammatory response following experimental brain injury. *Neurol. Res.* 25, 481–491.
- Shohami, E., Shapira, Y., Sidi, A., and Cotev, S. (1987). Head injury induces increased prostaglandin synthesis in rat brain. *J. Cereb. Blood Flow Metab.* 7, 58–63.
- Smith, P.K., Krohn, R.I., Hermanson, G.T., Mallia, A.K., Gartner, F.H., Provenzano, M.D., Fujimoto, E.K., Goeke, N.M., Olson, B.J., and Klenk, D.C. (1985). Measurement of protein using bicinchoninic acid. *Anal. Biochem.* 150, 76–85.
- Williams, J.F. (1991). Cytochrome P450 isoforms. Regulation during infection, inflammation and by cytokines. *J. Fla. Med. Assoc.* 78, 517–519.
- Xu, F., Falck, J.R., Ortiz de Montellano, P.R., and Kroetz, D.L. (2004). Catalytic activity and isoform-specific inhibition of rat cytochrome p450 4F enzymes. *J. Pharmacol. Exp. Ther.* 308, 887–895.
- Xu, J.A., Hsu, C.Y., Liu, T.H., Hogan, E.L., Perot, P.L., Jr, and Tai, H.H. (1990). Leukotriene B₄ release and polymorphonuclear cell infiltration in spinal cord injury. *J. Neurochem.* 55, 907–912.

Address reprint requests to:

Henry W. Strobel, Ph.D.

University of Texas-Houston Medical School

6431 Fannin Street

Houston, TX 77225

E-mail: henry.w.strobel@uth.tmc.edu